

Supporting information

Self-enhanced solid state electrochemiluminescence sensing platform SiO₂-PEI NPs and its application in the detection of spermine

Mathavan Sornambigai ^{a,b} Roselin Pavithra ^{a,b} Shekhar Handa ^{a,c} and Shanmugam Senthil Kumar ^{a,b} *

^aElectrodics and Electro Catalysis Division, CSIR-Central Electrochemical Research Institute (CSIR-CECRI), Karaikudi - 630 003, India

^bAcademy of Scientific and Innovative Research (AcSIR), Ghaziabad-201002, India

^cCorrosion and Material Protection Division, CSIR-CECRI, Karaikudi – 630 003, India.

***Corresponding author**

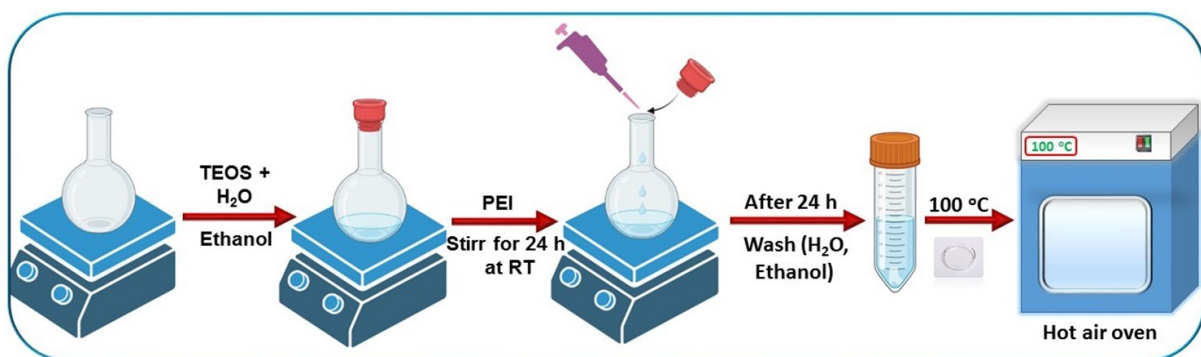
ssenthilmugam@gmail.com; ssenthilkumar@cecri.res.in

Table of Contents

S. No	CONTENTS
1.	Schematic representation for the synthesis of SiO₂-PEI NPs using stöber method..S-4
2.	Schematic representation of ink preparation for modifying GCE surface.....S-5
3.	Effect of pH.....S-6
4.	Control experiments.....S-7
4.	Effect of Scan rate.....S-8
5.	ECL Quenching mechanism in O₂ atmosphere.....S-9
5.	Chemical structure of spermine, spermidine, putrescine, and cadaverine.....S-10
6.	Oxidation reaction sequence of Spermine on the SiO₂-PEI NPs/[Ru(bpy)₃]²⁺/Nafion modified GCE electrode surface.....S-11
7.	XPS survey spectrum of SiO₂ NPs and SiO₂-PEI NPs.....S-12
8.	Table S1 showing geometric optimization of biogenic amines using DFT.....S-13
9.	Table S2 showing HOMO/LUMO of biogenic amines.....S-14
10.	Table S3 showing spin density data and plotsS-15
11.	Table S4 showing atomic charges and spin populations for molecules.....S-17
12.	Table S5 showing spin density of carbon radicals for biogenic amines.....S-20
13.	Table S6 showing atomic charges and spin populations.....S-21
14.	Table S7 showing buried volume at main amine radical site.....S-28

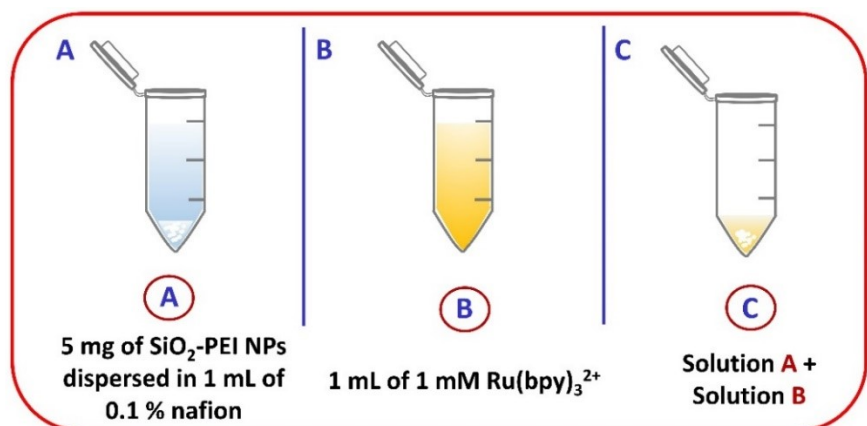
15.	Table S8 showing Buried volume at carbon radical site.....	S-29
16.	Table S9 Comparison of the developed system with other ECL methodologies for spermine detection.....	S-32
17.	Table S10 Quantification and recovery studies of spermine content in artificial urine sample using developed ECL detection method.....	S-33
18.	References.....	S-34

Schematic representation for the synthesis of SiO₂-PEI NPs using stöber method



Scheme S1. Schematic representation showing synthesis of SiO₂ NPs & SiO₂-PEI NPs via stÖber method;

Schematic representation of ink preparation for modifying GCE surface



Scheme S2. Steps involved in the ink preparation of SiO_2 PEI NPs- $[\text{Ru}(\text{bpy})_3]^{2+}$ /Nf modified GCE surface.

Control experiments

The CV and ECL intensity curves for $[\text{Ru}(\text{bpy})_3]^{2+}/\text{Nf}$ and SiO_2 PEI NPs- $[\text{Ru}(\text{bpy})_3]^{2+}/\text{Nf}$ modified GCE. As shown in the figure S2, the results suggest that the most effective enhancement in the ECL emission intensity was observed for the SiO_2 PEI NPs- $[\text{Ru}(\text{bpy})_3]^{2+}/\text{Nf}$ modified GCE. Therefore, we have chosen SiO_2 PEI NPs- $[\text{Ru}(\text{bpy})_3]^{2+}/\text{Nf}$ modified GCE for ECL experiments in the detection of spermine molecule. Also, in the case of SiO_2 PEI NPs- $[\text{Ru}(\text{bpy})_3]^{2+}/\text{Nf}$ modified GCE, PEI NPs in the SiO_2 PEI NPs matrix will act as a co-reactant accelerator, which plays crucial role in stabilizing the developed solid-state ECL sensing platform.

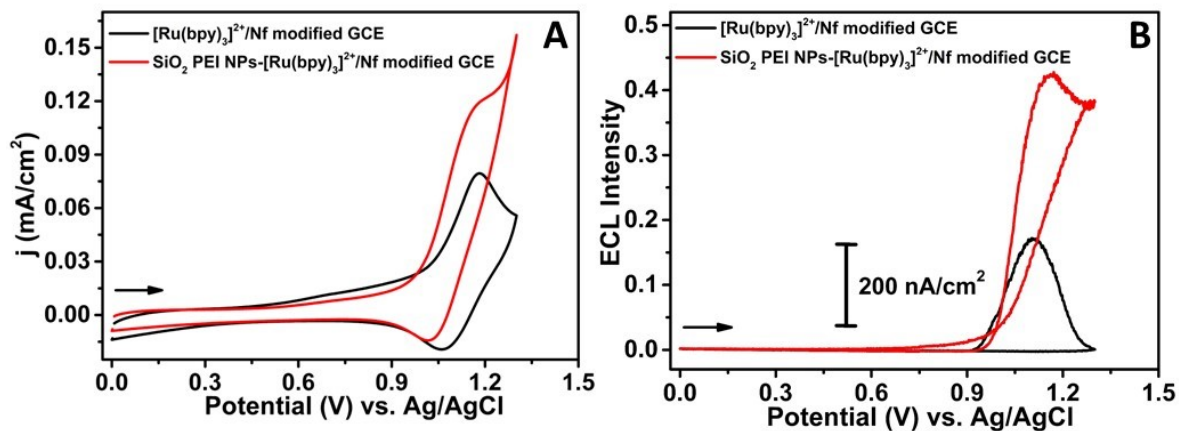


Figure S1. CV and ECL emission intensity plot of $[\text{Ru}(\text{bpy})_3]^{2+}/\text{Nf}$ modified GCE (black); and SiO_2 PEI NPs- $[\text{Ru}(\text{bpy})_3]^{2+}/\text{Nf}$ modified GCE (red) surface under N_2 -saturated 0.1 M PBS electrolyte, with the scan rate of 50 mV/s.

Effect of pH

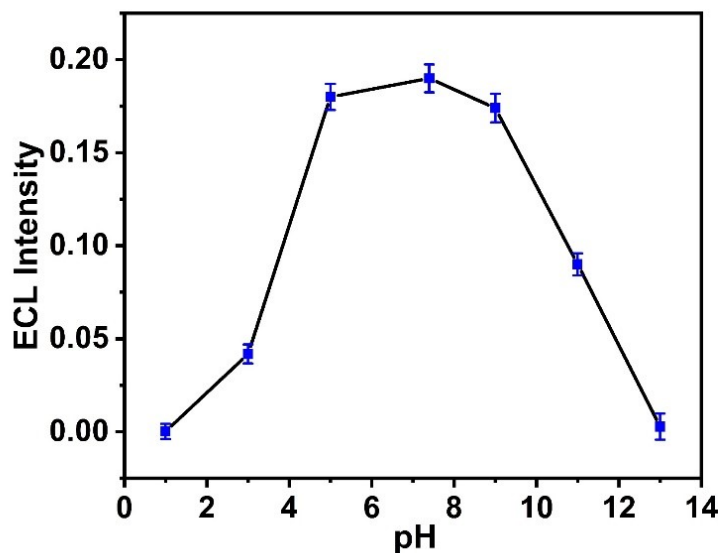


Figure S2. Derivative plot of ECL emission intensity recorded at a SiO_2 PEI NPs- $[\text{Ru}(\text{bpy})_3]^{2+}$ /Nf modified GCE surface under N_2 -saturated 0.1 M PBS electrolyte, with the scan rate of 50 mV/s.

The influence of pH on ECL emission intensity was also studied at a constant concentration of SiO_2 PEI NPs- $[\text{Ru}(\text{bpy})_3]^{2+}$ /Nf modified GCE under N_2 saturated 0.1 M PBS (pH 7.4) under cyclic voltammetric conditions, as shown in the Figure S2. The ECL of SiO_2 PEI NPs- $[\text{Ru}(\text{bpy})_3]^{2+}$ /Nf modified GCE is highly dependent on pH of the electrolyte solution. As seen from the Figure S1, the ECL emission diminishes in the $\text{pH} > 7.4$ and however, at pH greater than 7.4, the ECL emission decreases gradually. Therefore, the physiological pH value 7.4 was chosen as the optimum pH for all the experimental work.

Effect of Scan rate

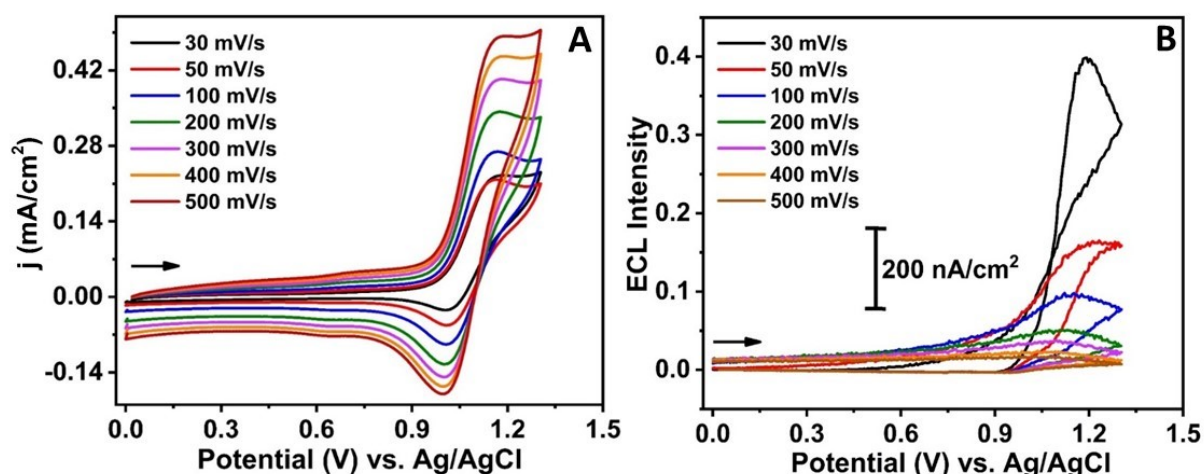


Figure S3. Shows the simultaneously recorded CV (A) and their ECL emission signals (B) in N_2 0.1 M PBS (pH 7.4) electrolyte at a SiO_2 PEI NPs-[Ru(bpy)₃]²⁺/Nf modified GCE surface under N_2 -saturated 0.1 M PBS electrolyte, at different scan rates.

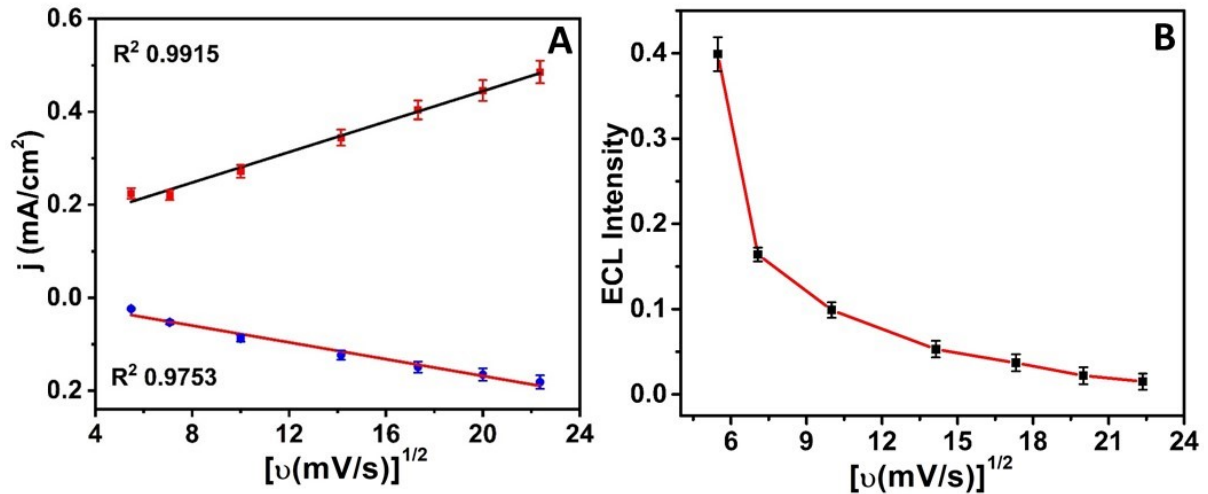
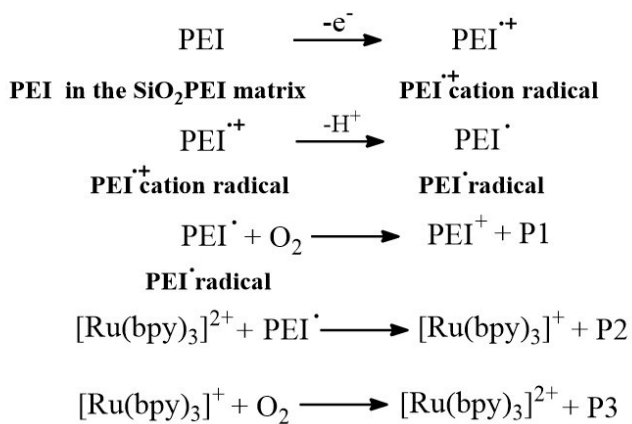


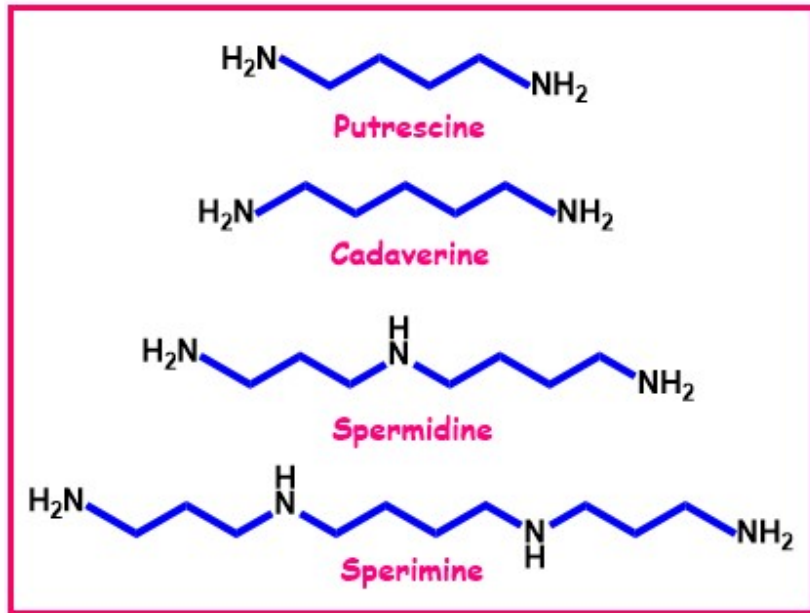
Figure S4. Linear plot for CV and their corresponding ECL signals recorded at a SiO_2 PEI NPs- $[\text{Ru}(\text{bpy})_3]^{2+}/\text{Nf}$ modified GCE surface under N_2 -saturated 0.1 M PBS electrolyte, at different scan rates.

ECL quenching mechanism in O_2 atmosphere

The ECL quenching mechanism behind the $[\text{Ru}(\text{bpy})_3]^{2+}$ chemically modified SiO_2 PEI matrix in the presence of dissolved oxygen (O_2) in the 0.1 M PBS electrolyte solution in the revised manuscript. Here, the formed $[\text{Ru}(\text{bpy})_3]^+$ reacts with the O_2 present in the electrolyte solution, which chemically produces the $[\text{Ru}(\text{bpy})_3]^{2+}$, without the formation of excited state $[\text{Ru}(\text{bpy})_3]^{2+*}$ [1, 2].

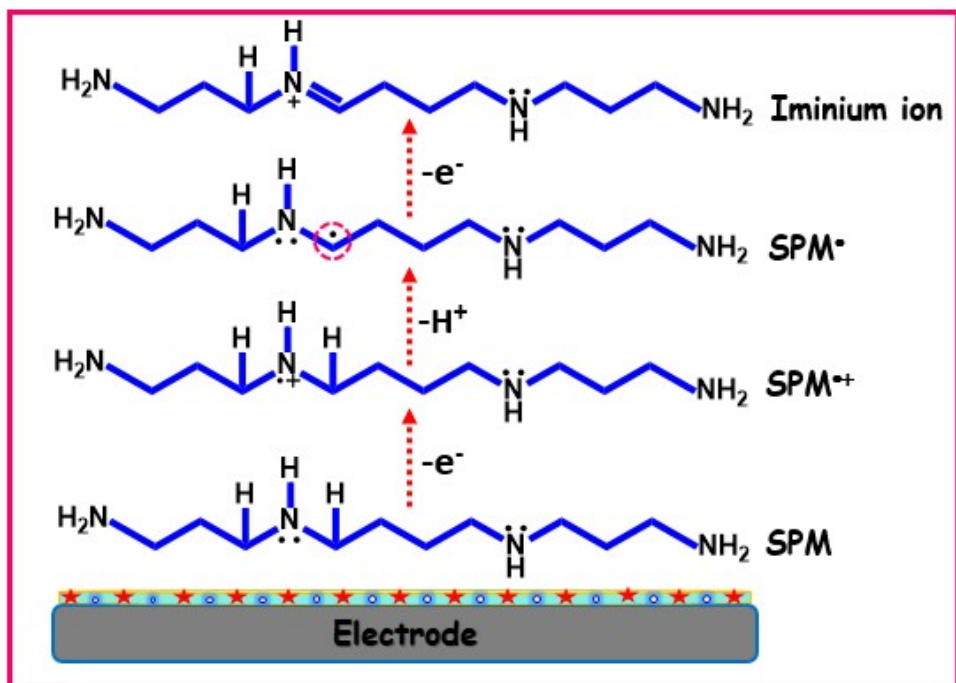


Chemical structure of spermine, spermidine, putrescine, and cadaverine



Scheme S3. Schematic representation showing the chemical structure of the biogenic amines such as putrescine, cadaverine, spermidine, and spermine.

Oxidation reaction sequence of Spermine on the $\text{SiO}_2\text{-PEI}$ NPs/ $[\text{Ru}(\text{bpy})_3]^{2+}$ /Nafion modified GCE electrode surface



Scheme S4. Proposed schematic representation showing spermine (SPM) oxidation reaction sequence at a SiO_2 PEI NPs- $[\text{Ru}(\text{bpy})_3]^{2+}$ /Nf modified GCE surface under N_2 -saturated 0.1 M PBS electrolyte with its abbreviations.

XPS survey spectrum of SiO_2 NPs and SiO_2 -PEI NPs

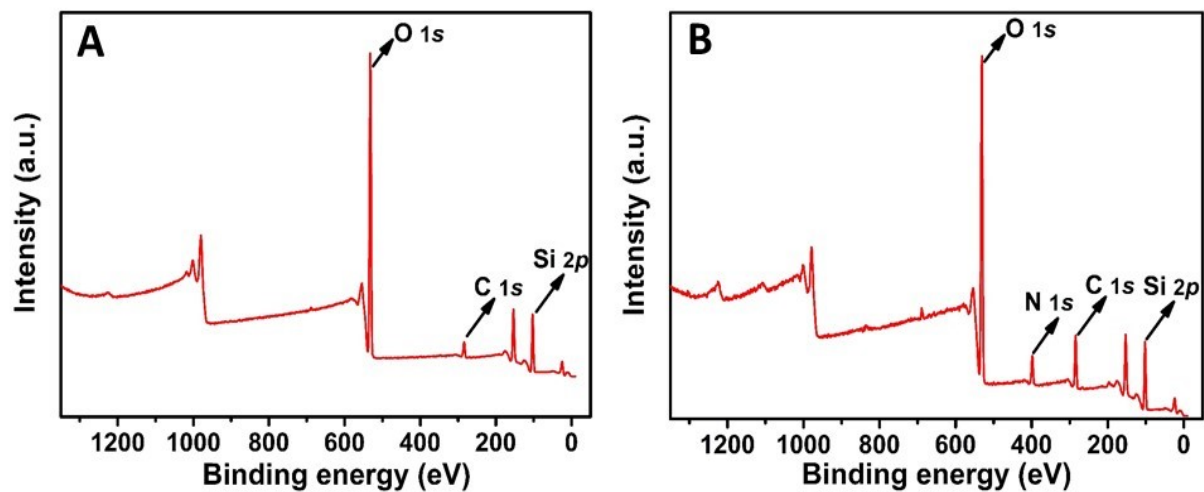
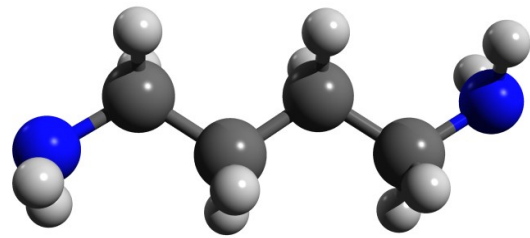


Figure S4. X-ray photoelectron spectroscopy (XPS) (a) survey spectrum of SiO_2 NPs; (b) survey spectrum of SiO_2 PEI NPs.

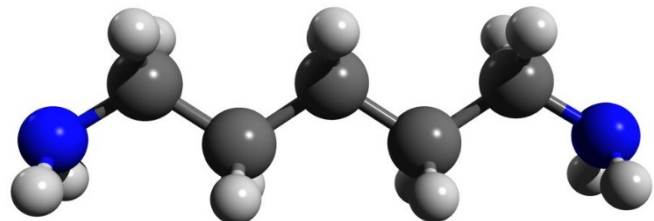
Geometric optimization of spermine, spermidine, putrescine, and cadaverine using DFT

Table S1: Optimized geometry (B3LYP-D4/TZVP level)

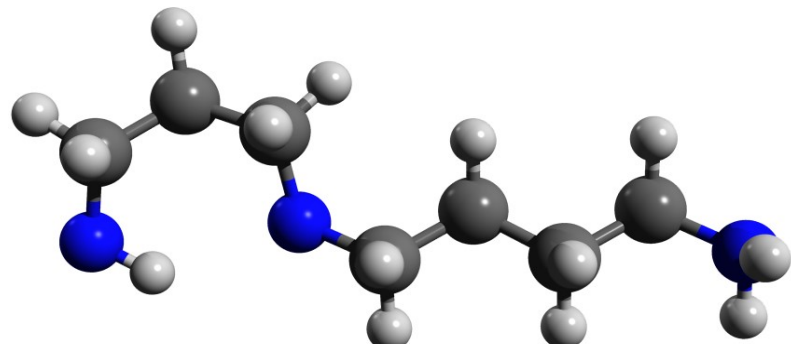
Putrascine



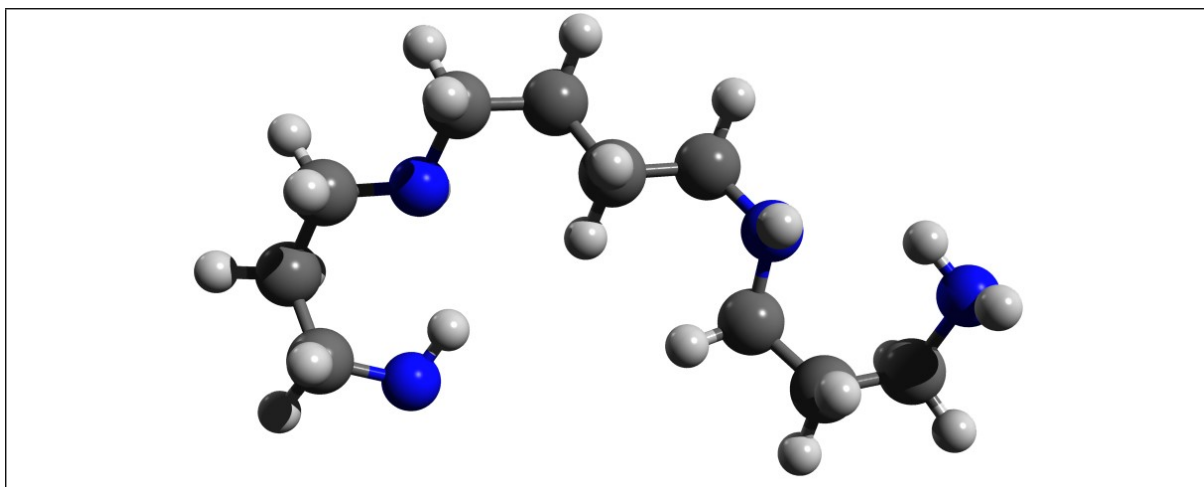
Cadavarine



Spermidine



Spermine

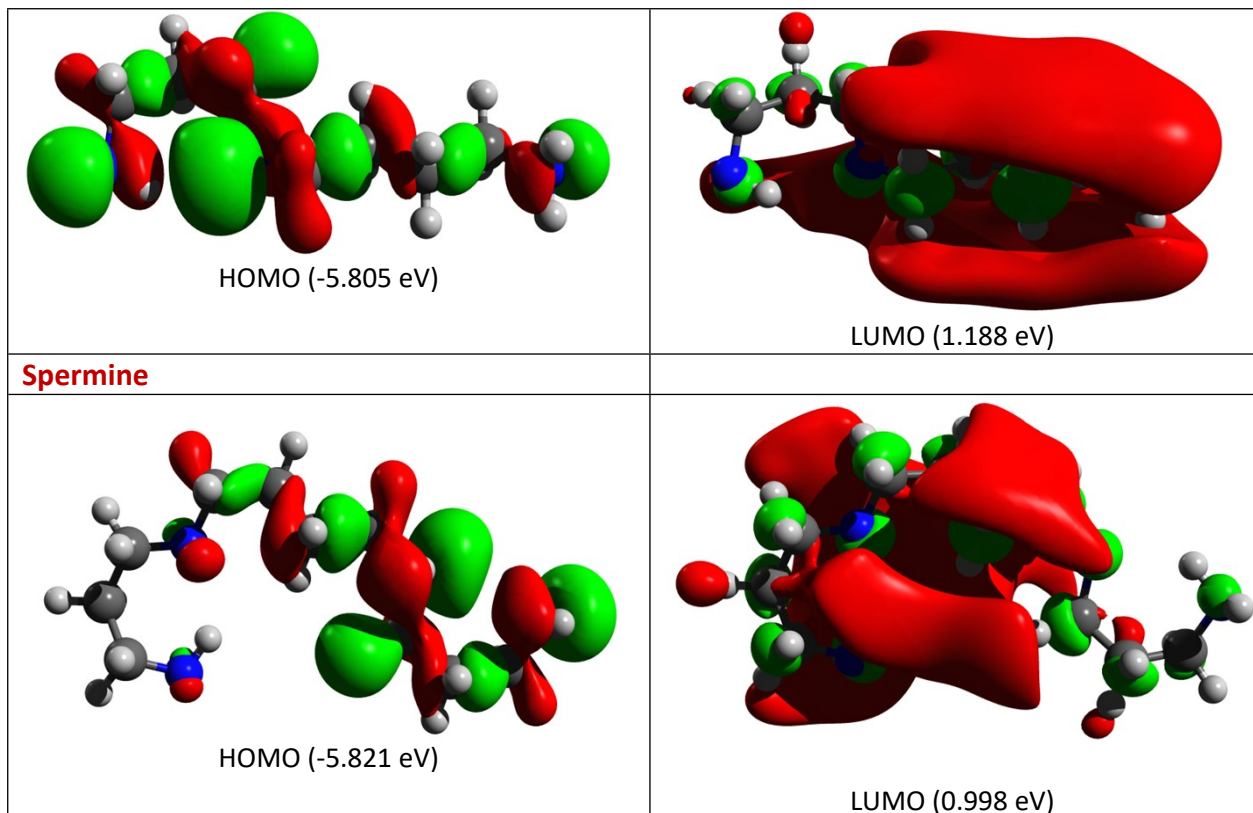


Images generated with Avogadro and POV-Ray [3, 4].

HOMO/LUMO of spermine, spermidine, putrescine, and cadaverine

Table S2: HOMO/LUMO of molecules [isovalue = 0.02]

Putrascine	
HOMO (-6.339 eV)	LUMO (1.077 eV)
Cadavarine	
HOMO (-6.371 eV)	LUMO (1.056 eV)
Spermidine	

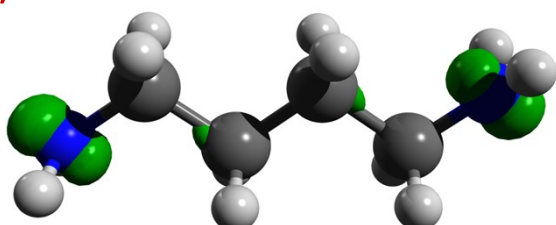


Images generated with Avogadro and POV-Ray.

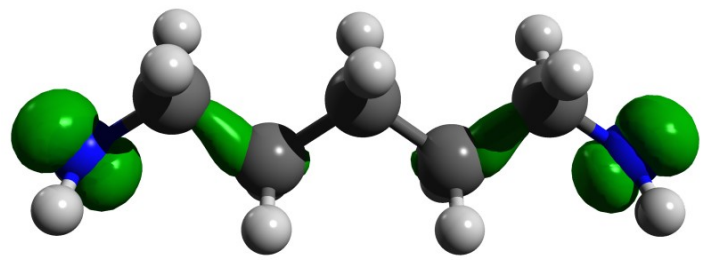
Spin density data and plots for spermine, spermidine, putrescine, and cadaverine

Table S3: Spin density plots (Isovalue = 0.02)

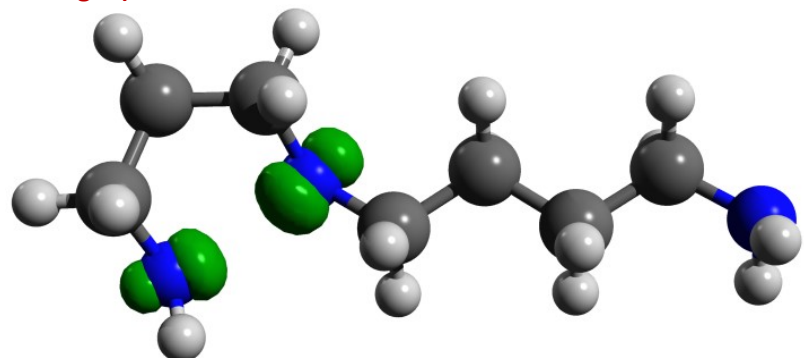
Putrescine (+1 charged)



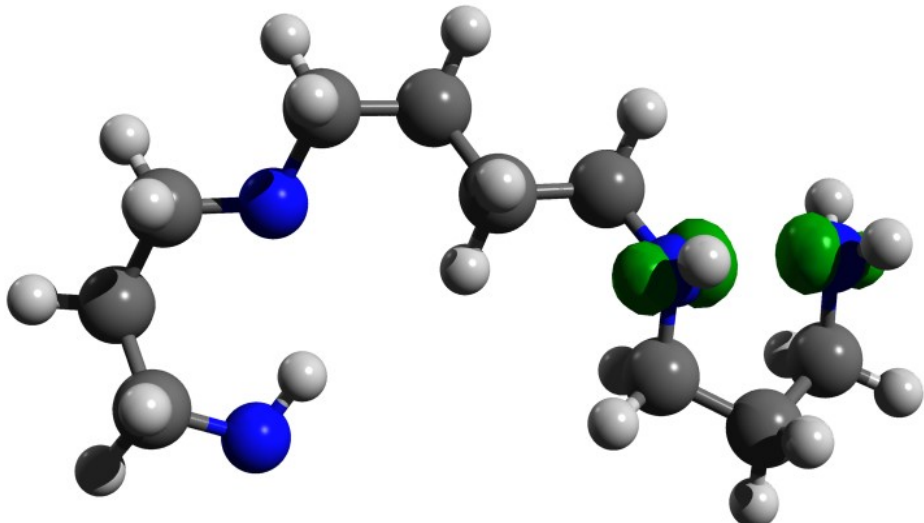
Cadavarine (+1 charged)



Spermidine (+1 charged)



Spermine (+1 charged)



Images generated with Avogadro and POV-Ray.

Atomic charges and spin populations for spermine, spermidine, putrescine, and cadaverine

Table S4: Atomic charges and spin populations for molecules

Putrascine

LOEWDIN ATOMIC CHARGES AND SPIN POPULATIONS

0 N :	0.049580	0.361823
1 C :	-0.286485	0.051451
2 H :	0.146886	0.003586
3 H :	0.146880	0.003573
4 C :	-0.227772	0.070978
5 H :	0.148629	0.000136
6 H :	0.148626	0.000135
7 C :	-0.227778	0.070973
8 H :	0.148623	0.000135
9 H :	0.148627	0.000137
10 C :	-0.286498	0.051445
11 H :	0.146880	0.003581
12 H :	0.146878	0.003578
13 N :	0.049532	0.361750
14 H :	0.186846	0.004179
15 H :	0.186845	0.004179
16 H :	0.186849	0.004180
17 H :	0.186852	0.004181

Cadaverine

LOEWDIN ATOMIC CHARGES AND SPIN POPULATIONS

0 C :	-0.289800	0.050082
1 C :	-0.230989	0.069050
2 H :	0.145824	-0.000198
3 H :	0.145814	-0.000206
4 C :	-0.235820	0.033434
5 H :	0.146044	-0.000176
6 H :	0.146046	-0.000176
7 C :	-0.230944	0.069106
8 H :	0.145816	-0.000205
9 H :	0.145823	-0.000196
10 C :	-0.289787	0.050140
11 H :	0.145723	0.004081
12 H :	0.145712	0.004062
13 N :	0.039347	0.348421
14 H :	0.185196	0.004137

15 H :	0.185189	0.004139
16 N :	0.039091	0.348110
17 H :	0.145693	0.004058
18 H :	0.145701	0.004067
19 H :	0.185162	0.004134
20 H :	0.185159	0.004134

Spermidine

LOEWDIN ATOMIC CHARGES AND SPIN POPULATIONS

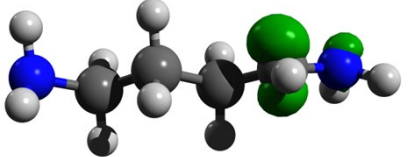
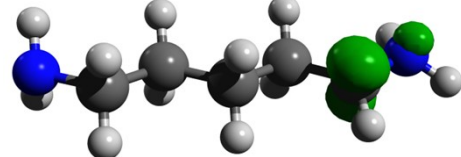
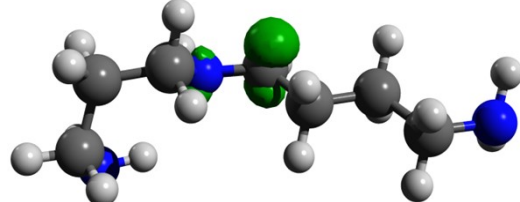
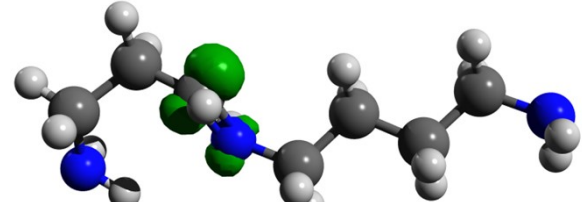
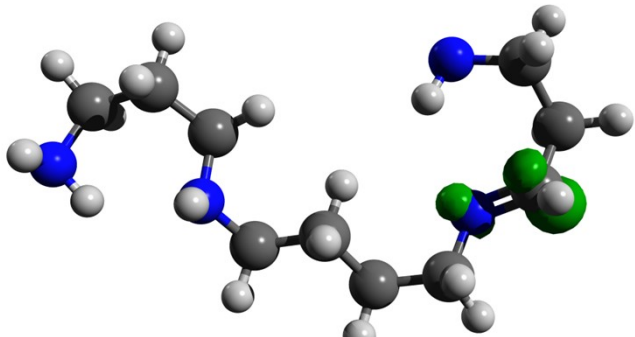
0 H :	0.140637	0.000922
1 H :	0.147111	-0.000309
2 C :	-0.254941	0.046944
3 C :	-0.306711	0.031435
4 C :	-0.244784	0.037424
5 N :	-0.037002	0.243320
6 H :	0.145854	0.008746
7 H :	0.154177	-0.000395
8 C :	-0.335234	0.009255
9 C :	-0.261127	0.013802
10 H :	0.138126	0.000427
11 H :	0.138072	-0.000006
12 C :	-0.240379	0.044926
13 H :	0.144788	0.000810
14 H :	0.144996	-0.000242
15 C :	-0.263651	0.039499
16 H :	0.151829	0.006843
17 H :	0.149889	0.002216
18 N :	0.197308	0.420421
19 H :	0.214051	0.004775
20 H :	0.172583	0.044350
21 H :	0.166476	0.003327
22 H :	0.176771	0.002547
23 H :	0.130934	0.000137
24 H :	0.130963	0.000127
25 N :	-0.169567	0.033936
26 H :	0.156974	0.000354
27 H :	0.157186	0.000392
28 H :	0.154668	0.004019

Spermine

LOEWDIN ATOMIC CHARGES AND SPIN POPULATIONS

0 H :	0.128236	0.000218
1 H :	0.134605	-0.000033
2 C :	-0.304059	0.005745
3 C :	-0.343595	0.004861

4 C :	-0.271276	0.004725
5 N :	-0.172582	0.042532
6 H :	0.127944	0.001111
7 H :	0.139916	0.000141
8 C :	-0.270539	0.033063
9 C :	-0.246921	0.036998
10 H :	0.139859	0.000322
11 H :	0.143340	-0.000301
12 C :	-0.251669	0.008689
13 H :	0.143585	0.000069
14 H :	0.141313	-0.000068
15 C :	-0.297284	0.014648
16 H :	0.136225	0.001426
17 H :	0.130608	0.011864
18 N :	0.016659	0.063973
19 H :	0.181845	0.000711
20 H :	0.124311	0.005972
21 H :	0.144185	0.000511
22 H :	0.153493	0.000322
23 H :	0.148053	0.005119
24 H :	0.147588	0.002310
25 N :	0.174055	0.375513
26 H :	0.135532	0.001006
27 H :	0.173460	0.002246
28 H :	0.152081	-0.000372
29 H :	0.143386	0.007784
30 N :	-0.056316	0.215940
31 C :	-0.311490	0.027883
32 C :	-0.248536	0.033149
33 C :	-0.261090	0.041674
34 H :	0.163862	0.003013
35 H :	0.145328	-0.000281
36 H :	0.138853	0.000816
37 H :	0.209416	0.004391
38 H :	0.165531	0.038753
39 H :	0.152088	0.003555

Table S5: Spin density plots for carbon radicals (Isovalue = 0.02)	Radical stabilization energy (Kcal/mol)
Putrascine 	13.44913
Cadavarine 	13.45222
Spermidine Radical 1 	14.70367
Radical 2 	17.00095
Spermine Radical 1 	16.26578

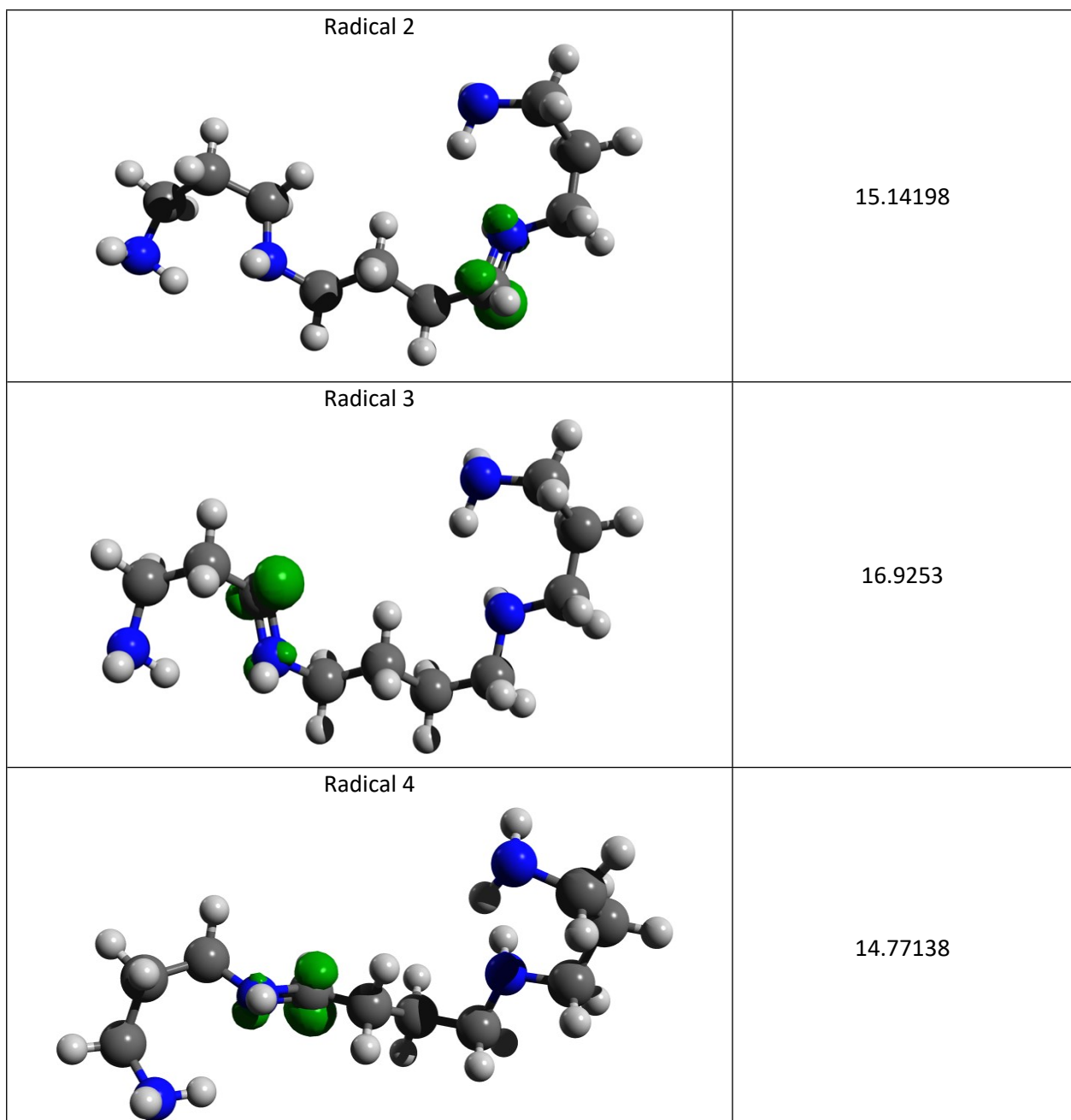


Table S6: ATOMIC CHARGES AND SPIN POPULATIONS

Putrascine

LOEWDIN ATOMIC CHARGES AND SPIN POPULATIONS

0 N : -0.192173 0.063899

1 C : -0.234932 0.785333

2 H : 0.119289 0.007492

3 C : -0.288238 0.063033

4 H :	0.136001	0.005920
5 H :	0.141873	0.033020
6 C :	-0.279996	0.002561
7 H :	0.132223	-0.000198
8 H :	0.131905	0.001114
9 C :	-0.340725	0.000413
10 H :	0.126941	0.000025
11 H :	0.126849	0.000511
12 N :	-0.201934	-0.000067
13 H :	0.152572	0.000047
14 H :	0.152531	0.000003
15 H :	0.162486	0.034139
16 H :	0.155327	0.002758

Cadavarine

LOEWDIN ATOMIC CHARGES AND SPIN POPULATIONS

0 C :	-0.235144	0.785240
1 C :	-0.289281	0.063125
2 H :	0.135517	0.005923
3 H :	0.141446	0.033172
4 C :	-0.264314	0.002433
5 H :	0.135076	-0.000192
6 H :	0.134731	0.001155
7 C :	-0.279663	0.000388
8 H :	0.131649	0.000041
9 H :	0.131552	0.000486
10 C :	-0.340318	0.000013
11 H :	0.126487	0.000011
12 H :	0.126523	0.000054
13 N :	-0.202838	-0.000094
14 H :	0.152335	0.000010
15 H :	0.152348	-0.000002
16 N :	-0.192717	0.063811
17 H :	0.119010	0.007563
18 H :	0.155240	0.002742
19 H :	0.162362	0.034120

Spermidine

Radical 1

LOEWDIN ATOMIC CHARGES AND SPIN POPULATIONS

0 H :	0.126025	0.000042
1 H :	0.133365	0.000270
2 C :	-0.309312	0.008869

3 C :	-0.340261	0.000206
4 C :	-0.279594	0.001571
5 N :	-0.211262	0.000037
6 H :	0.126307	0.000032
7 H :	0.140741	-0.000148
8 C :	-0.341120	0.000442
9 C :	-0.279461	0.002372
10 H :	0.132159	-0.000215
11 H :	0.132338	0.001106
12 C :	-0.279177	0.062941
13 H :	0.136689	0.005820
14 H :	0.143226	0.032755
15 C :	-0.204458	0.779184
16 H :	0.121460	0.006420
17 N :	-0.020835	0.063493
18 H :	0.180253	0.030603
19 H :	0.119091	0.001551
20 H :	0.136215	-0.000109
21 H :	0.149800	0.000020
22 H :	0.126950	0.000030
23 H :	0.126850	0.000512
24 N :	-0.201977	-0.000075
25 H :	0.152515	0.000005
26 H :	0.152712	0.000045
27 H :	0.130761	0.002220

Radical 2

LOEWDIN ATOMIC CHARGES AND SPIN POPULATIONS

0 H :	0.125535	0.001546
1 H :	0.140859	0.031351
2 C :	-0.209066	0.759342
3 C :	-0.340627	0.009297
4 C :	-0.294565	0.049170
5 N :	-0.209936	0.001624
6 H :	0.126620	0.000497
7 H :	0.141168	0.001758
8 C :	-0.340754	0.000069
9 C :	-0.277444	0.000038
10 H :	0.132122	0.000055
11 H :	0.132595	0.000027
12 C :	-0.269954	0.002313
13 H :	0.133533	-0.000056
14 H :	0.133746	0.000202
15 C :	-0.313993	0.008298
16 H :	0.130675	0.001454
17 H :	0.130268	0.002585

18 N :	-0.013259	0.077804
19 H :	0.180263	0.030881
20 H :	0.119552	0.021977
21 H :	0.136441	-0.000508
22 H :	0.149886	0.000217
23 H :	0.126791	0.000006
24 H :	0.126775	0.000001
25 N :	-0.202221	0.000050
26 H :	0.152414	0.000001
27 H :	0.152576	0.000001

Spermine

Radical 1

LOEWDIN ATOMIC CHARGES AND SPIN POPULATIONS

0 H :	0.123136	0.001687
1 H :	0.135691	0.005826
2 C :	-0.315684	0.617804
3 C :	-0.337545	0.035670
4 C :	-0.305326	0.056777
5 N :	-0.199117	0.004589
6 H :	0.124271	0.006120
7 H :	0.141960	0.004565
8 C :	-0.314513	0.000348
9 C :	-0.272402	0.003265
10 H :	0.129945	0.001458
11 H :	0.133335	0.000095
12 C :	-0.263587	0.000046
13 H :	0.139443	0.000090
14 H :	0.137434	-0.000093
15 C :	-0.289354	0.019742
16 H :	0.134889	0.001932
17 H :	0.120187	0.012903
18 N :	0.058333	0.211374
19 H :	0.185290	0.007255
20 H :	0.119140	0.007599
21 H :	0.142806	0.000704
22 H :	0.152595	0.000058
23 H :	0.128928	0.000121
24 H :	0.130313	0.000022
25 N :	-0.023386	0.000001
26 H :	0.149129	-0.000000
27 H :	0.139974	0.000001
28 H :	0.125860	-0.000000
29 N :	-0.212562	-0.000000
30 C :	-0.340731	0.000000

31 C :	-0.279738	0.000002
32 C :	-0.309956	0.000036
33 H :	0.134992	-0.000002
34 H :	0.132812	0.000000
35 H :	0.125665	0.000000
36 H :	0.170604	0.000001
37 H :	0.116485	0.000002
38 H :	0.130683	0.000001

Radical 2

LOEWDIN ATOMIC CHARGES AND SPIN POPULATIONS

0 H :	0.127187	0.000002
1 H :	0.134595	-0.000082
2 C :	-0.291974	0.019351
3 C :	-0.338905	0.000917
4 C :	-0.277362	-0.000047
5 N :	-0.205578	0.005165
6 H :	0.127239	0.000010
7 H :	0.141940	0.000067
8 C :	-0.316320	0.003938
9 C :	-0.268562	0.033713
10 H :	0.129806	-0.000232
11 H :	0.130417	0.000768
12 C :	-0.289152	0.055391
13 H :	0.140681	0.002638
14 H :	0.138499	0.007496
15 C :	-0.310820	0.628325
16 H :	0.118978	0.008213
17 N :	0.058047	0.201727
18 H :	0.186142	0.007326
19 H :	0.120493	0.013019
20 H :	0.139367	0.004518
21 H :	0.151133	0.000492
22 H :	0.129025	0.000054
23 H :	0.130034	0.000019
24 N :	-0.023621	0.004069
25 H :	0.135500	0.001921
26 H :	0.149226	0.000016
27 H :	0.139938	0.000027
28 H :	0.125870	0.000002
29 N :	-0.212613	0.000148
30 C :	-0.340928	0.000030
31 C :	-0.279782	0.000036
32 C :	-0.309793	0.000400

33 H :	0.134952	0.000162
34 H :	0.132828	0.000001
35 H :	0.125598	0.000003
36 H :	0.170549	0.000084
37 H :	0.116672	0.000300
38 H :	0.130692	0.000012

Radical 3

LOEWDIN ATOMIC CHARGES AND SPIN POPULATIONS

0 H :	0.125861	0.000001
1 H :	0.132850	-0.000000
2 C :	-0.310841	0.000031
3 C :	-0.340566	0.000018
4 C :	-0.279224	0.000009
5 N :	-0.210897	0.000078
6 H :	0.125998	0.000003
7 H :	0.140180	0.000003
8 C :	-0.303323	0.015248
9 C :	-0.271143	0.012310
10 H :	0.130374	0.002607
11 H :	0.134073	-0.000117
12 C :	-0.264229	0.000694
13 H :	0.138330	0.000467
14 H :	0.136307	0.000009
15 C :	-0.308103	0.000642
16 H :	0.130128	-0.000001
17 H :	0.115813	0.000081
18 N :	-0.023216	0.000155
19 H :	0.173340	0.000011
20 H :	0.115310	0.000005
21 H :	0.136608	-0.000014
22 H :	0.149469	0.000007
23 H :	0.131445	0.000460
24 H :	0.132891	0.000720
25 N :	0.026261	0.183659
26 H :	0.130057	0.000002
27 H :	0.151485	0.000099
28 H :	0.140572	0.002312
29 H :	0.128062	0.005161
30 N :	-0.204425	0.009032
31 C :	-0.337178	0.029507

32 C :	-0.306084	0.051707
33 C :	-0.268895	0.658918
34 H :	0.139972	0.003770
35 H :	0.133436	0.002515
36 H :	0.126300	0.000292
37 H :	0.181219	0.006377
38 H :	0.121782	0.013220

Radical 4

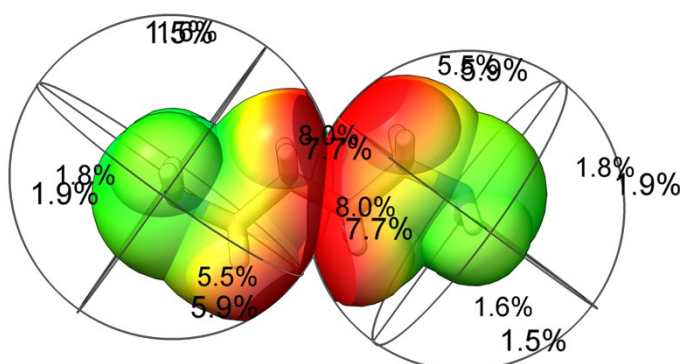
LOEWDIN ATOMIC CHARGES AND SPIN POPULATIONS

0 H :	0.125906	-0.000001
1 H :	0.132901	-0.000000
2 C :	-0.310613	0.000473
3 C :	-0.340436	0.000013
4 C :	-0.279181	-0.000003
5 N :	-0.210961	0.000054
6 H :	0.126047	0.000004
7 H :	0.140250	0.000008
8 C :	-0.219631	0.751535
9 C :	-0.283559	0.066647
10 H :	0.139382	0.030152
11 H :	0.136599	0.005097
12 C :	-0.266800	0.003524
13 H :	0.137760	0.001478
14 H :	0.135994	-0.000123
15 C :	-0.309040	-0.000507
16 H :	0.130086	0.000026
17 H :	0.115738	-0.000147
18 N :	-0.022951	0.003251
19 H :	0.173526	0.000090
20 H :	0.115545	0.000147
21 H :	0.136482	0.000200
22 H :	0.149575	-0.000003
23 H :	0.119819	0.005864
24 N :	-0.015499	0.085535
25 H :	0.130145	0.000015
26 H :	0.150065	0.000110
27 H :	0.141762	0.001011
28 H :	0.126657	-0.000033
29 N :	-0.210169	0.001750
30 C :	-0.339832	0.000471
31 C :	-0.278289	0.003085

32 C :	-0.303167	0.036313
33 H :	0.136989	0.000693
34 H :	0.133987	-0.000087
35 H :	0.126290	0.000034
36 H :	0.173892	0.001019
37 H :	0.121069	0.001286
38 H :	0.133663	0.001019

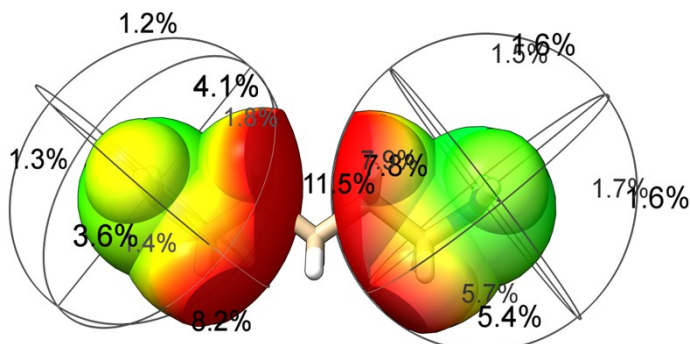
Table S7: Buried volume at main amine radical site

Putrescine



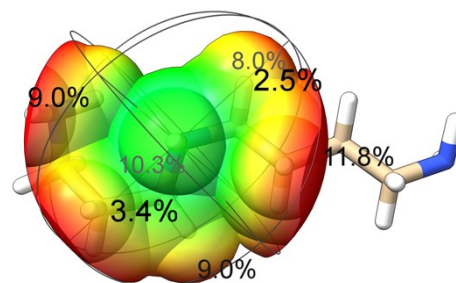
% Buried volume at radical centre = 33.8

Cadavarine

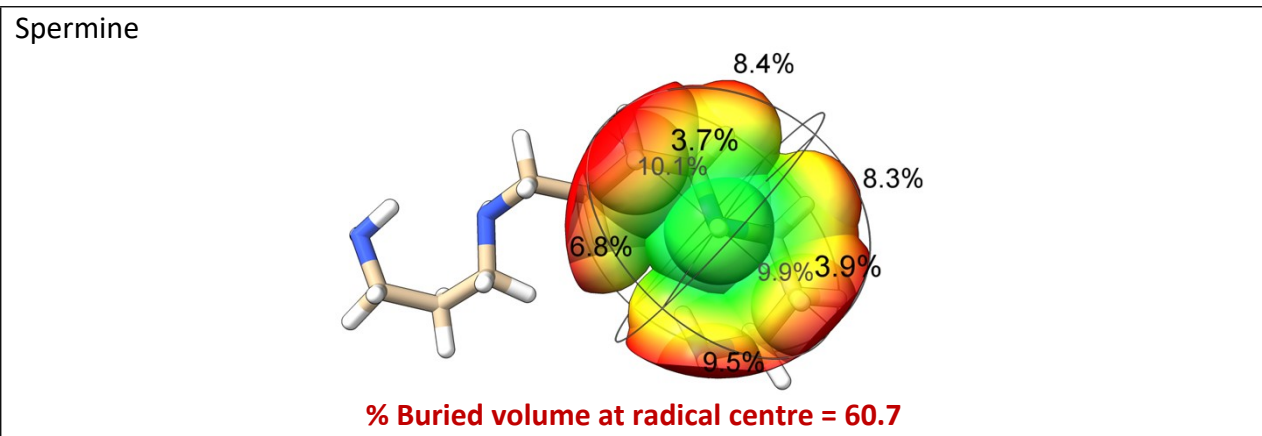


% Buried volume at radical centre = 33.2

Spermidine

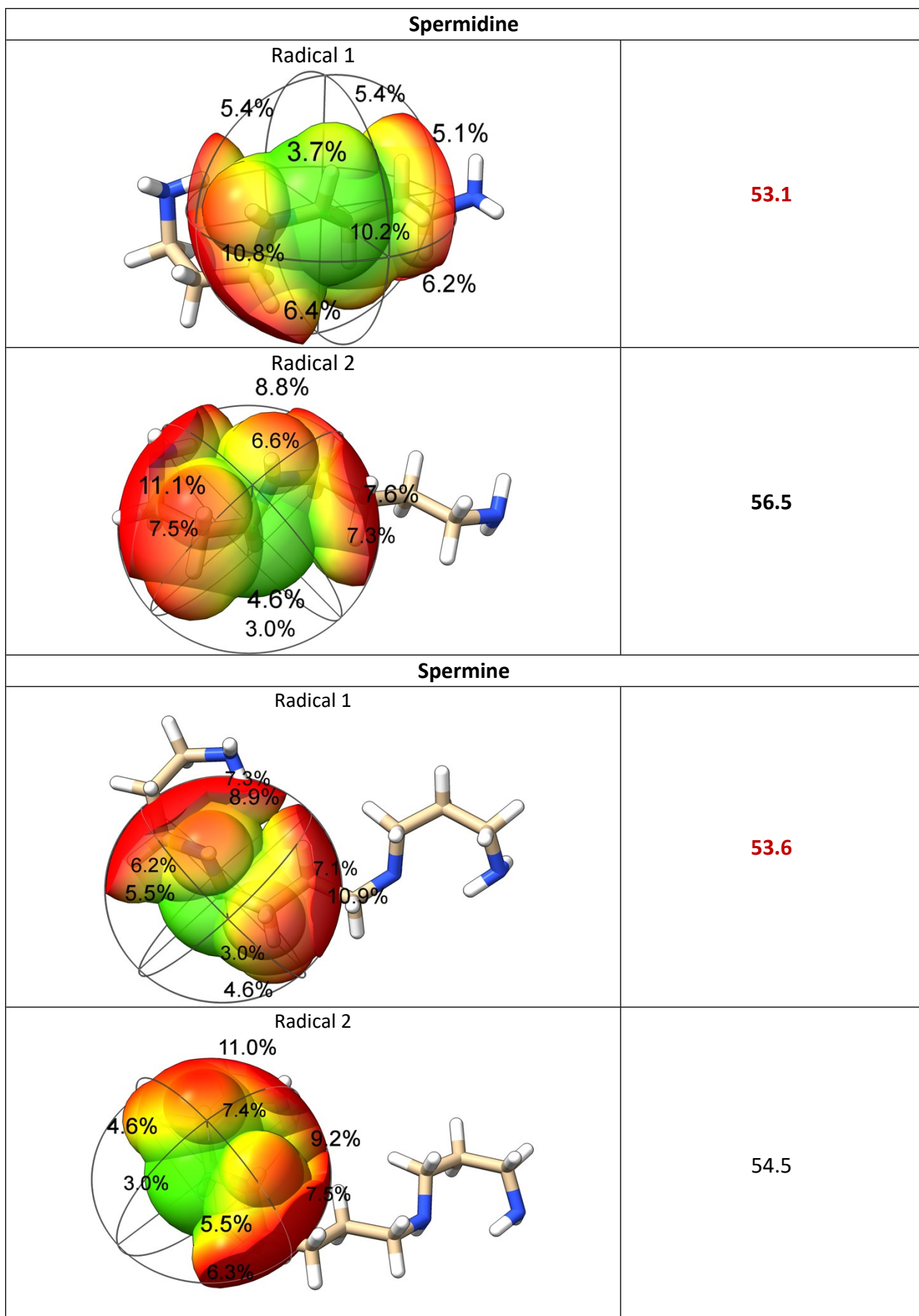


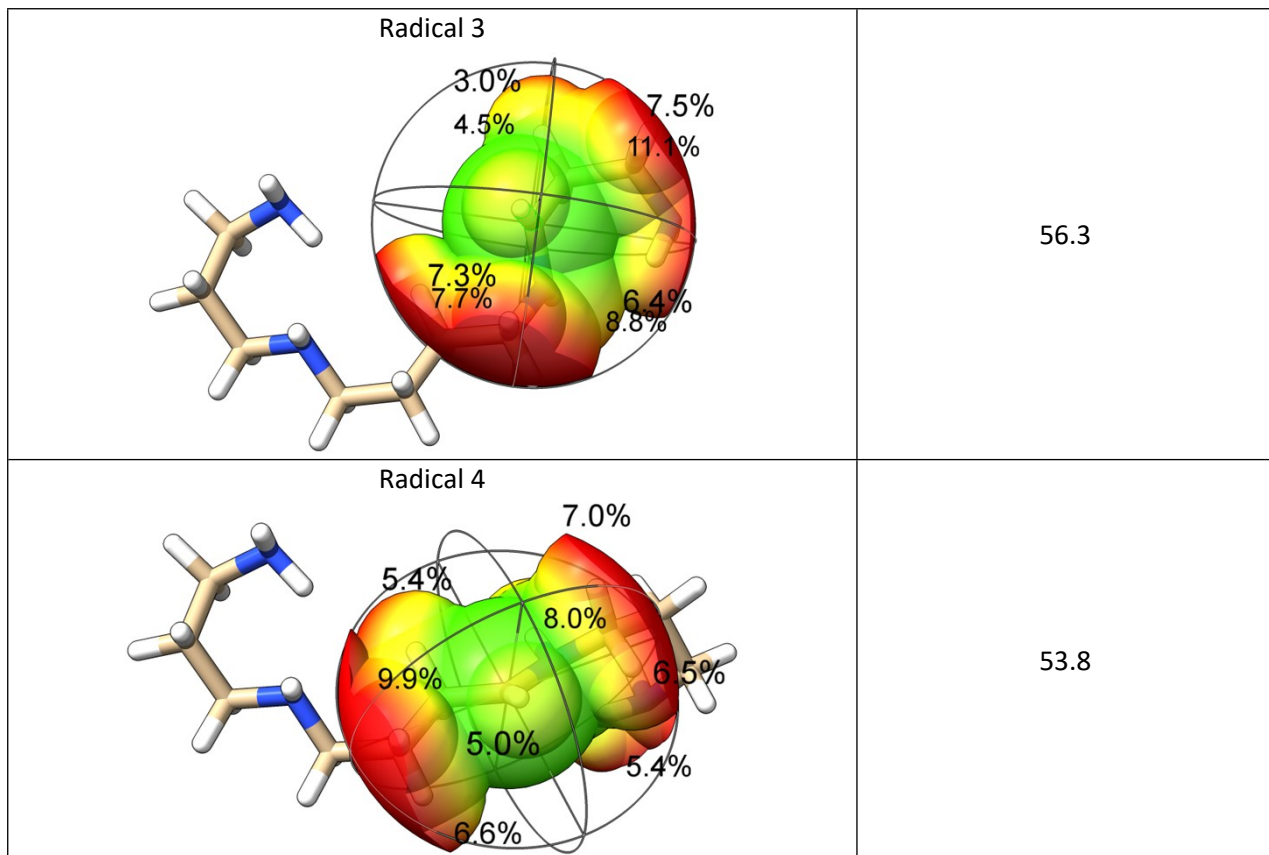
% Buried volume at radical centre = 56.5



Images generated with chimera and buried volume calculated using SEQCROW.

Table S8: Buried volume at carbon radical site	% Buried volume at radical centre (% V _{bur})
Putrascine	44.6
Cadavarine	44.4





Images generated with chimera and buried volume calculated using SEQCROW [5].

Table S9. Comparison of the developed system with other ECL methodologies for spermine detection

S. no.	Analytical method	Linear range	LOD	Ref.
1.	ECL-CE	0.25 μM – 0.5 μM	0.2 μM	[6]
2.	Electrochemical analysis	3 μM to 300 μM	1 μM	[7]
3.	Luminescence analysis	5 μM to 0.5 mM	0.5 μM	[8]
4.	Solid-state ECL method	10 nM to 100 nM	12.2 nM	This work

Table S10. Quantification and recovery studies of spermine content in urine sample using developed ECL detection method.

Sample No.	Original content (10^{-9} M)	Added (10^{-9} M)	Found (10^{-9} M)	Recovery (%)	<i>t</i>-test
1.	13.2	10 nM	13.3±0.004	105 %	0.495
2.		30 nM	20.6±0.001	93.5 %	0.012
3.		50 nM	49.6±0.12	86.4 %	0.866

References

- [1] Zheng, H.; Zu, Y. Emission of Tris(2,2'-Bipyridine)Ruthenium(II) by Coreactant Electrogenerated Chemiluminescence: From O₂-Insensitive to Highly O₂-Sensitive. *J. Phys. Chem. B* 2005, 109 (24), 12049–12053. <https://doi.org/10.1021/jp050350d>.
- [2] Gross, E. M.; Pastore, P.; Wightman, R. M. High-Frequency Electrochemiluminescent Investigation of the Reaction Pathway between Tris(2,2'-Bipyridyl)Ruthenium(II) and Tripropylamine Using Carbon Fiber Microelectrodes. *J. Phys. Chem. B* 2001, 105 (37), 8732–8738. <https://doi.org/10.1021/jp011434z>.
- [3] (a) Parkinson, C. J.; Mayer, P. M.; Radom, L. *Theor. Chem. Acc.* 1999, 102, 92. <https://doi.org/10.1007/s002140050477>; (b) Parkinson, C. J.; Mayer, P. M.; Radom, L. *J. Chem.Soc., Perkin Trans. 2* 1999, 11, 2305. <https://doi.org/10.1039/A905476F>.
- [4] S. S. V. Sowndarya, P. C. St. John, R. S. Paton, *Chem. Sci.* 2021, 12, 13158–13166. <https://doi.org/10.1039/D1SC02770K>.
- [5] (a) A. J. Schaefer, V. M. Ingman, and S. E. Wheeler, "SEQCROW: A ChimeraX Bundle to Facilitate Quantum Chemical Applications to Complex Molecular Systems" *J. Comp. Chem.* 42, 1750 (2021). <https://doi.org/10.1002/jcc.26700>; (b) V. M. Ingman, A. J. Schaefer, L. R. Andreola, and S. E. Wheeler, "QChASM: Quantum Chemistry Automation and Structure Manipulation" *WIREs Comp. Mol. Sci.* 11, e1510 (2021). <https://doi.org/10.1002/wcms.1510>.
- [6] H. Li, X. Liu, W. Niu, S. Zhu, L. Fan, L. Shi and G. Xu, "CEC with tris (2,2'-bipyridyl) ruthenium (II) electrochemiluminescent detection" *Electrophoresis*, 2008, **29**, 4475–4481.

- [7] A. Boffi, G. Favero, R. Federico, A. Macone, R. Antiochia, C. Tortolini, G. Sanzó and F. Mazzei, “Amine oxidase-based biosensors for spermine and spermidine determination” *Anal. Bioanal. Chem.*, 2015, **407**, 1131–1137.
- [8] Z. Hu and B. Yan, Deep Learning-Assisted Intelligent Artificial Vision Platform Based on Dual-Luminescence Eu(III)-Functionalized HOF for the Diagnosis of Breast and Ovarian Cancer *Anal. Chem.*, 2023, **95**, 18889–18897.